ELSEVIER

Journal of Alloys and Compounds 334 (2002) 211–218

Journal of ALLOYS AND COMPOUNDS

www.elsevier.com/locate/jallcom

Synthesis and luminescence properties of oxyapatite $NaY_9Si_6O_{26}$ doped with Eu^{3+}, Tb^{3+}, Dy^{3+} and Pb^{2+}

X.H. Chuai[a,b], H.J. Zhang[b,*], F.Sh. Li[a], Sh.Z. Lu[c], J. Lin[b], Sh.B. Wang[b], Kou. Chi-Chou[a]

[a]*Science and Technology University of Beijing, Beijing 100081, People's Republic of China*

[b]*Laboratory of Rare Earth Chemistry and Physics, Changchun Institute of Applied Chemistry, Chinese Academy of Sciences, Changchun 130022, People's Republic of China*

[c]*Laboratory of Excited State Processes, Changchun Institute of Optics, Fine Mechanic and Physics Chinese Academy of Sciences, Changchun 130000, People's Republic of China*

Received 11 January 2001; received in revised form 28 April 2001; accepted 25 June 2001

Abstract

Oxyapatite $NaY_9Si_6O_{26}$ was prepared by sol–gel method. By choosing the precursors, a single phase compound was obtained. This soft chemical method lowered the reaction temperature by 100°C compared with the solid state method. Its morphology was studied by transmission electron microscopy (TEM). Several rare earth ions (Eu^{3+}, Tb^{3+}, Dy^{3+}) and Pb^{2+} ion were doped in this compound. The high resolution emission spectrum of Eu^{3+} showed that rare earth ions occupied two yttrium sites. In spite of the charge imbalance of Pb^{2+} with the cations in this compound, it was found that Pb^{2+} could emit in UV range and transfer its excitation energy to Dy^{3+} ion.

Keywords: Phosphor; Sol–gel

1. Introduction

Sol–gel synthesis method has many advantages over the conventional solid state methods, i.e. it offers better homogeneity and lowers sintering temperature, etc. With the same activator concentration, luminescence materials prepared by the former method have higher brightness than those by the latter method because of the better dispersion of activator and less non-radiative relaxation [1]. Some silicate phosphors such as Zn_2SiO_4:Mn^{2+} and Y_2SiO_5:Tb^{3+} have been made by this method [2,3]. Apatite structure is versatile. By changing anions and cations, many isostructural compounds can be obtained. Among them, some present better matrices for phosphors [4,5]. The luminescence properties of a few silicate oxyapatites doped with rare earth ions have been reported [6]. In this paper, another silicate oxyapatite $NaY_9Si_6O_{26}$ was prepared by the sol–gel method. The reactants were mixed at molecule or nanoscale level. The change of the microstructure in the precursor might occur when different reactants were used, which affected the phase development. Single phase oxypatite $NaY_9Si_6O_{26}$ doped with Eu^{3+}, Tb^{3+}, Dy^{3+} and Pb^{2+} ions were prepared by selecting the reactants, and their luminescence properties were investigated.

2. Experimental

2.1. Preparation of the samples

Rare earth ions (Eu^{3+}, Dy^{3+}, Tb^{3+}) oxides were dissolved in dilute nitric acid (HNO_3) and mixed with stoichiometric amounts of sodium acetate (NaAc) and 3-glycidoxypropyl-trimethoxysilane (GPTMS,$C_9H_{20}O_5Si$). Then, the mixture was put in an oven at 65°C to increase the rate of hydrolysis and condensation of GPTMS and to slowly remove the excessive water. The organic group connected to silicon had a better compatibility with NaAc. If $NaNO_3$ was used in place of NaAc, precipitation would occur in the above procedure. At around 200°C, the organic group in GPTMS carbonated which gave off a large amount of heat and inflated the precursors. For

*Corresponding author.

E-mail address: zhgroup@ciac.cn (H.J. Zhang).

0925-8388/02/$ – see front matter
PII: S0925-8388(01)01758-3

comparison, another silicate source tetraethoxysilane $Si(OC_2H_5)_4$ (TEOS) was used in place of GPTMS. To get the polycrystalline, these powders were heat-treated at 900°C and 1000°C for 6 h, respectively.

2.2. Measurement

The heat-treated powders were characterized using a D/Max-II powder X-ray diffractometer using Cu as radiative source (λ_1=0.15405 nm). The morphology was studied by transmission electron microscope (TEM). Luminescence (excitation and emission) spectra were measured using a SPEX FL-2T2 spectrofluorometer. High resolution spectra were measured using forth harmonics of Nd:YAG laser at 266 nm. The UV-visible absorption spectrum was measured using a XF-1 spectrophotometer.

3. Results and discussion

3.1. Phase of sol–gel derived powders

The calcinated powders was not a single phase, but a mixture of Y_2SiO_5 and $NaY_9Si_6O_{26}$ if the TEOS was used as silicon source. The X-ray diffraction patterns of the powders heat-treated at 1000°C were shown in Fig. 1(a). To remove the phase of Y_2SiO_5, GPTMS was selected as silicon source. From Ref. [7], it was reported that the powder Y_2SiO_5 prepared by using TEOS and $Y(NO_3)_3$ as precursors crystallized at 900°C. However, Y_2SiO_5 derived from GPTMS and $Y(NO_3)_3$ crystallized at 1000°C and crystallization of Y_2SiO_5 at lower temperature was hampered. In fact, when NaAc, GPTMS and $Y(NO_3)_3$ were mixed at the stoichiometric ratio, the derived powder sintered at 1000°C had the single phase $NaY_9Si_6O_{26}$ and its X-ray diffraction pattern is shown in Fig. 1(b). The use of GPTMS changed the mid-phase of the product resulting in the pure phase $NaY_9Si_6O_{26}$. TEM analysis revealed that the powder shape was irregular and the size was in the range 50–100 nm, as shown in Fig. 2.

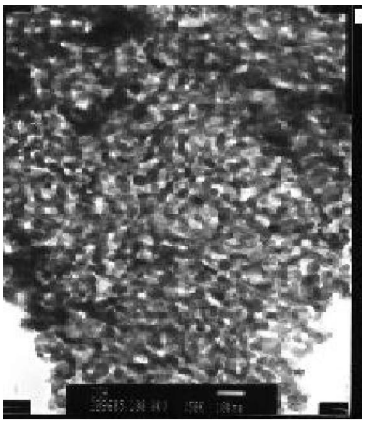

Fig. 2. TEM photograph of the $NaY_9Si_6O_{26}$ powder (sintered for 10 h).

3.2. Site of the doped Eu^{3+} ion

The crystallographic structures of silicate apatites have been investigated [8]. It is reported that there are two different Ln^{3+} sites with unequal coordination number, viz. 4*f* site having nine coordination with the symmetry of C_3 (I site) and 6*h* site having seven coordination with the symmetry of *Cs* (II site). Generally, the splitting number of

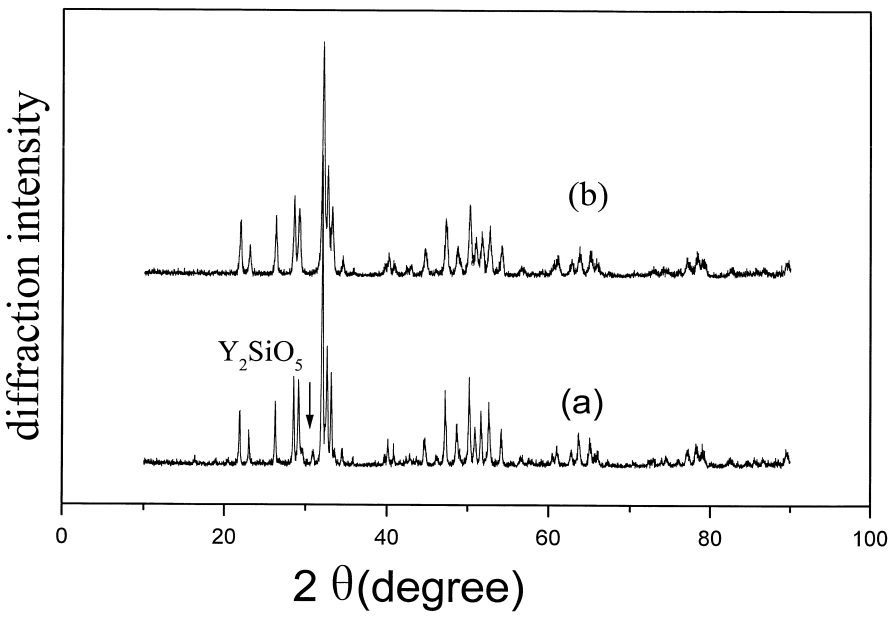

Fig. 1. X-ray diffraction patterns of the powders sintered at 1000°C, (a) derived from TEOS and $Y(NO_3)_3$ and $NaNO_3$, (b) derived from GPTMS and $Y(NO_3)_3$ and NaAc.

the states ^7F_J of Eu^{3+} depends on the site symmetry and the J value with the maximum of $2J+1$. $^5D_0$ and $^7F_0$ are not split at any environment and the number of the emission lines from the $^5D_0-^7F_0$ transition corresponds to the site number of different Eu^{3+} ions. So Eu^{3+} ion is used as fluorescence structure probe in many fields. The high resolution emission spectrum of $NaY_9Si_6O_{26}:Eu^{3+}$ is shown in Fig. 3. There exists only one emission line for the transition of $^5D_0-^7F_0$, but five for $^5D_0-^7F_1$ (17074.1, 16843.5, 16820.5, 16740.5, 16705.6 cm^{-1}), which is more than the maximum number of three for the transition of $^5D_0-^7F_1$. The above result indicates that Eu^{3+} ions occupy two yttrium sites (6*h* and 4*f*) in this compound. There is only one line for the transition of $^5D_0-^7F_0$, which may be ascribed to the much weaker intensity from another site.

3.3. Fluorescence spectra of Tb^{3+}, Dy^{3+}

Fig. 4(a) shows the luminescence spectra of $NaY_9Si_6O_2:Tb^{3+}$ (0.3at.%). The emission (excited at 237 nm) from the higher level $^5D_3$ was prominent. When the concentration of Tb^{3+} was increased, the transition from $^5D_3$ exited state decreased and that from $^5D_4$ level dominated (shown in Fig. 4(b)). The following cross-relaxation (shown in Eq. (1)) may occur resulting in the relaxation of $^5D_3$ to $^5D_4$. The excitation spectrum of Tb^{3+} (monitored at λ_{em}=544 nm) includes f–d and f–f transitions. For a Tb^{3+} ion, the transition of f–d includes two bands, the spin-allowed transition at shorter wavelength with more intensity and the spin-forbidden at longer wavelength with the weaker intensity.

$$Tb^{3+}(^5D_3) + Tb^{3+} \rightarrow (^7F_6)Tb^{3+}(^5D_4) + Tb^{3+}(^7F_0) \quad (1)$$

Dy^{3+} can give blue and yellow emission corresponding to the $^4F_{9/2}-^6H_{15/2}$ and $^4F_{9/2}-^6H_{13/2}$ transitions, respectively. The transition $^4F_{9/2}-^6H_{13/2}$ with $L=2$, $\Delta J=2$ is hypersensitive and its emission intensity depends on Dy^{3+} ion's surroundings. By suitably adjusting the yellow-to-blue intensity ratio (Y/B), one can get white color luminescence materials activated by Dy^{3+} in one matrix. Dy^{3+} ion doped in $NaY_9Si_6O_{26}$ can emit white light with $Y/B=1.007$. Its luminescence spectra are shown in Fig. 5. When Dy^{3+} ion was doped in $NaGd_9Si_6O_{26}$, its excitation spectrum contained the characteristic transition of Gd^{3+} ion, viz, $^6I-^8S$ at 274 nm, $^6P-^8S$ at 313 nm and $^6D-^8S$ at 260 nm indicating the energy transfer from Gd^{3+} to Dy^{3+}.

3.4. UV–visible absorption spectrum and fluorescence spectra of Pb^{2+}

Pb^{2+} has the $6S^2$ electron configuration and it is often used as an activator or a sensitizer. Its absorption in the ultraviolet is due to the transition of $sp-s^2$ transition. The interaction between orbit and spin splits the p electron level into four states of $^3P_0$, $^3P_1$, $^3P_2$ and $^1P_1$, in the sequences of increasing energy level. The transition of

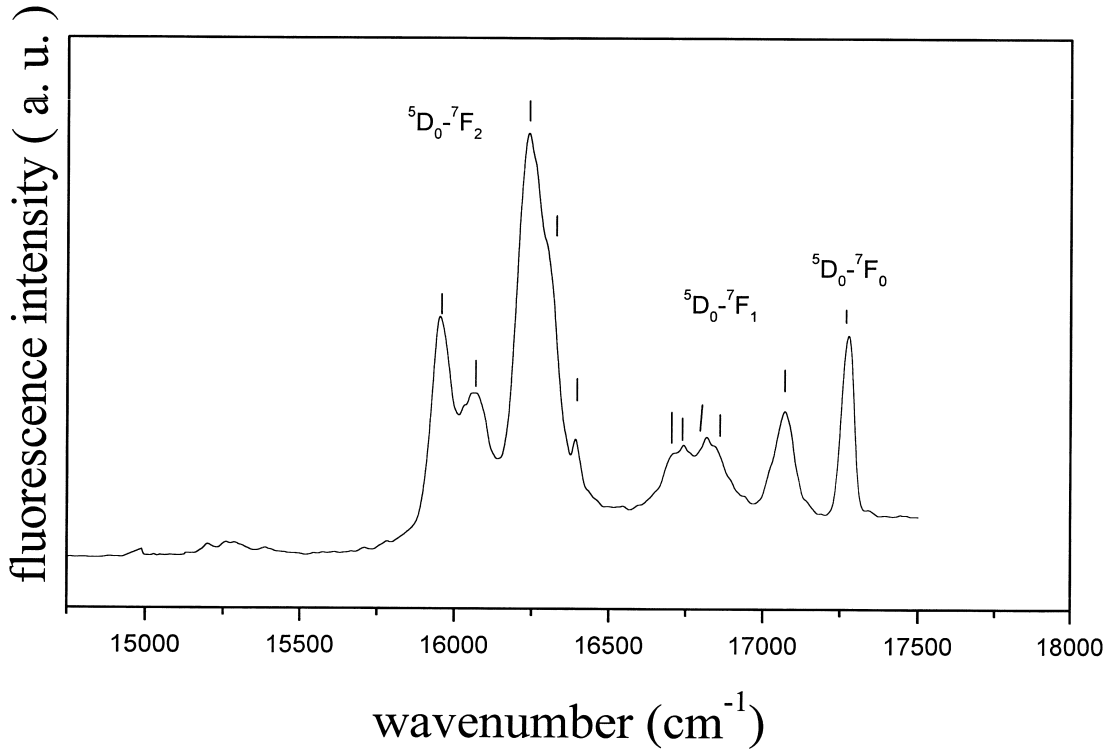

Fig. 3. High resolution emission spectrum of $NaY_9Si_6O_{26}:Eu^{3+}$ (1.4at.%).

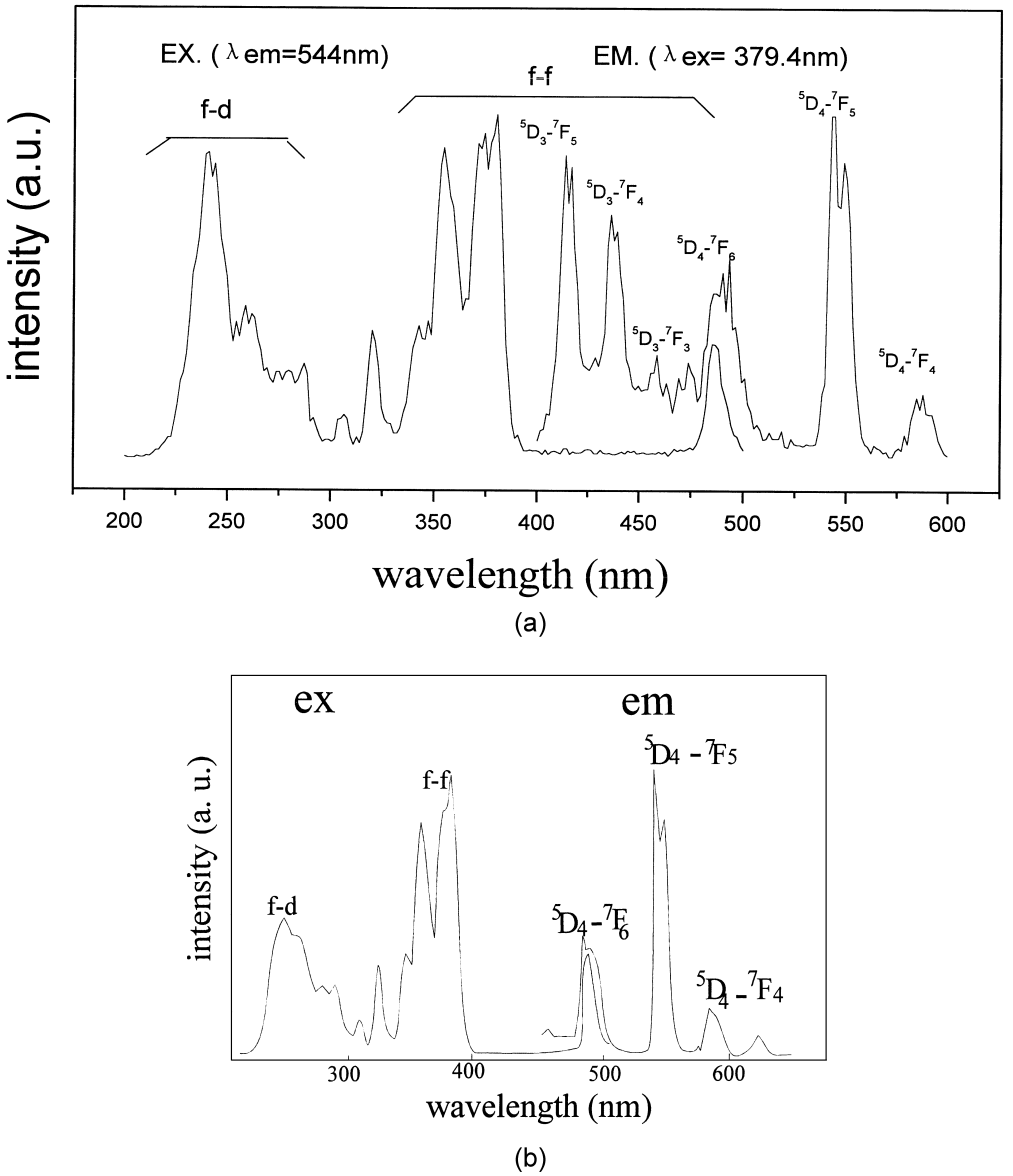

Fig. 4. Fluorescence spectra of $NaY_9Si_6O_{26}$ doped with (a) 0.3at.% Tb^{3+} and (b) 1.395at.% Tb^{3+}, the excitation spectra were monitored at $\lambda_{em}=544$ nm and the emission spectra at $\lambda_{ex}=380$ nm.

$^1S_0\rightarrow{}^1P_1$ is the spin permitted one having the strong absorption. However, the transition of $^1S_0\rightarrow{}^3P_1$ can be also observed due to the spin–orbit couple mixing the spin triplet and singlet states. The absorption spectrum of $Na_{(1-x)}Pb_xY_9Si_6O_{26}$ is shown in Fig. 6. Its shape is asymmetric and can be deconvoluted into two peaks (232.8 and 270.9 nm). The matrix had not absorption in this range and those two bands were originated from the Pb^{2+} ion. So the two peaks were assigned to $^1S_0\rightarrow{}^1P_1$ and $^1S_0\rightarrow{}^3P_1$, respectively. The energy difference between the two bands is 7000 cm^{-1} which is usual for Pb^{2+} ion [9]. Its luminescence spectra are shown in Fig. 7. the excitation spectrum monitored at 382 nm emission is coincident with the absorption spectrum and the excitation band is assigned to $^1S_0\rightarrow{}^3P_1$ transition and the transition of $^1S_0\rightarrow{}^1P_1$ was undetectable by the instrument. When Pb^{2+} was doped in series compounds of $NaLn_9SiO_6O_{26}$ (Ln=Y, La, Gd) occupying Na sites, the emission wavelengths of these Pb^{2+} ions had a great difference and were listed in Table 1 with radius of rare earth ions.

Pb^{2+} ion was doped in $NaY_9Si_6O_{26}$ in the form of $NaY_{9(1-x)}Pb_xSi_6O_{26}$ and its fluorescence spectra are shown in Fig. 8. Its excitation spectrum was a broad band peaking at 277 nm with a weak shoulder at 322 nm (monitored by the emission of 389 nm). When the sample was excited at 322 nm, its emission spectrum had a red shift (centered at 415 nm). This difference of emission spectra indicated that there existed two sites for Pb^{2+} ions. There are two yttrium

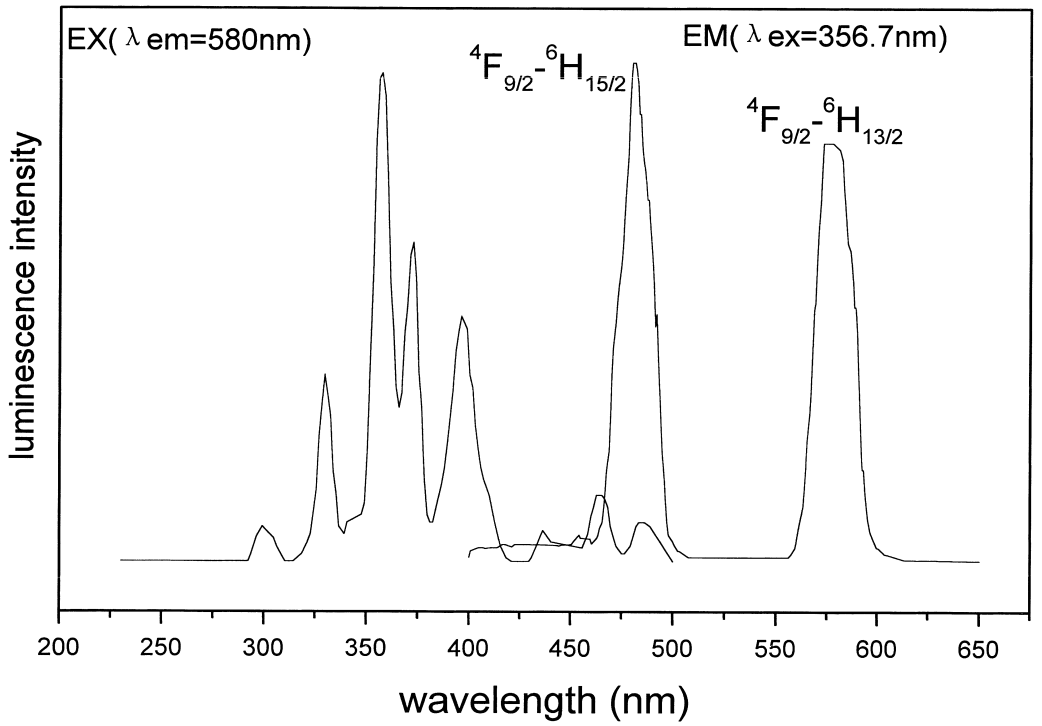

Fig. 5. Excitation and emission spectra of Dy^{3+} doped $NaY_{9(1-x)}Dy_{9x}Si_6O_{26}$ ($x=0.014$).

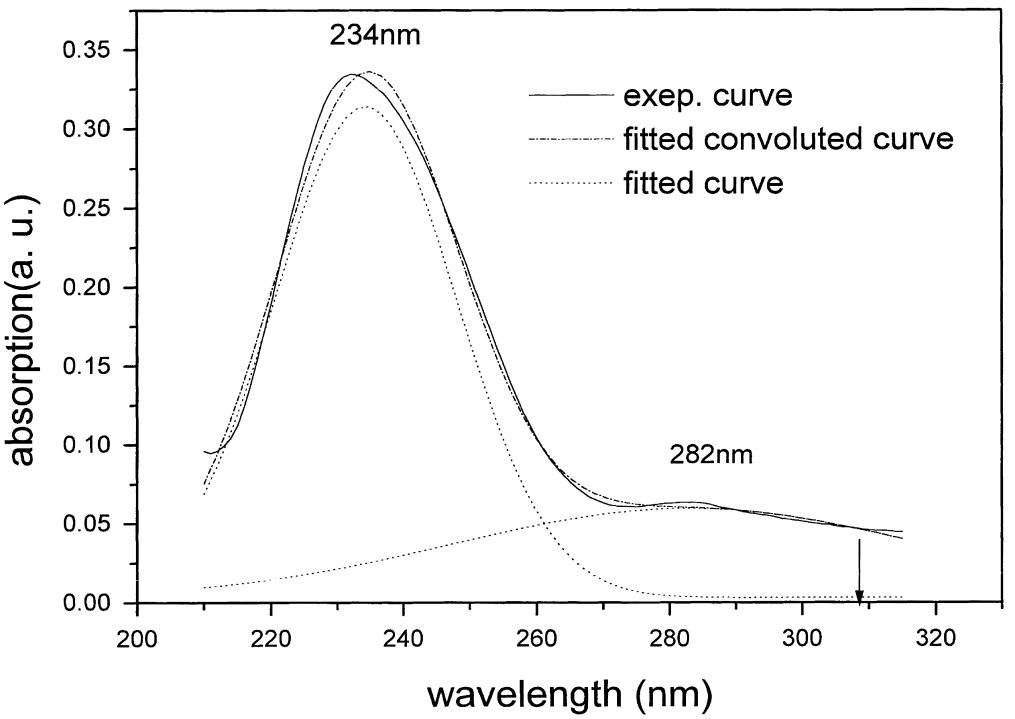

Fig. 6. Absorption spectrum of $Na_{(1-x)}Pb_xY_9Si_6O_{26}$ ($x=0.1$).

sites in $NaY_9Si_6O_{26}$ and the longer wavelength emission was assigned to that from site II coordinated by the 'free oxygen' which increased the covalency.

In gadolinium compounds, the activators trap the energy migrating over the gadolinium sublattice. The spectra of Pb^{2+} doped in $NaGd_9Si_6O_{26}$ are shown in Fig. 9. The excitation spectrum contained the lines of ^8S–^6I at 274 nm and ^8S–^6P at 313 nm of Gd^{3+} proving the energy transfer

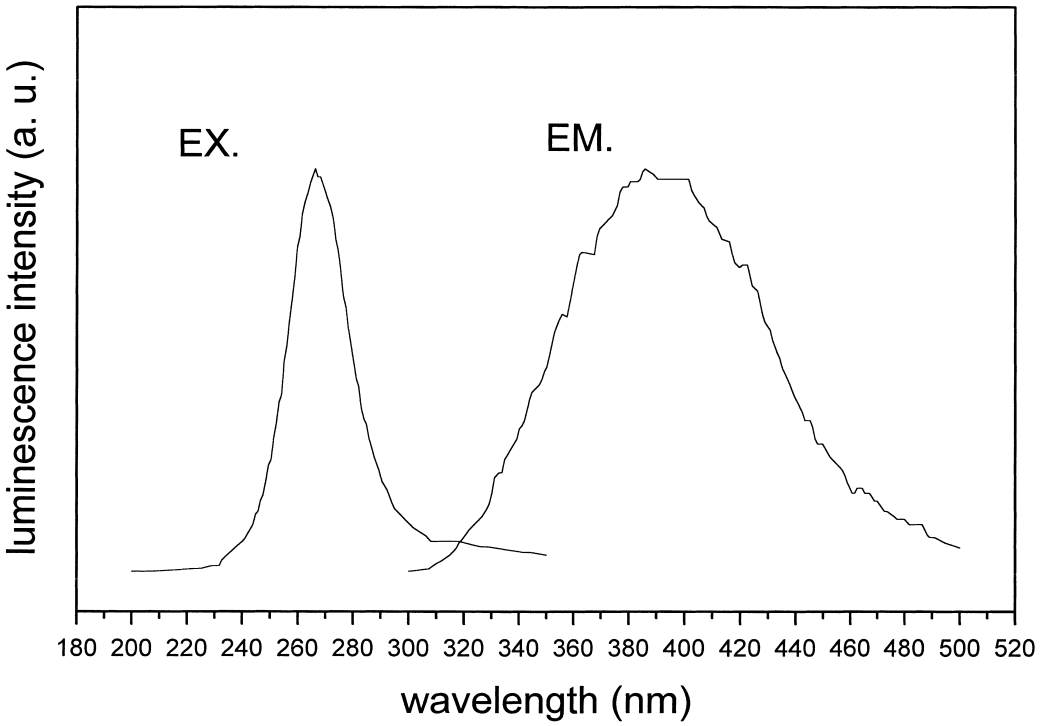

Fig. 7. Excitation and emission spectra of $Na_{(1-x)}Pb_xY_9Si_6O_{26}$ ($x=0.1$).

from Gd^{3+} to Pb^{2+} ion. When excited at 274 nm, there appeared the emission band of Pb^{2+} and the emission at 313 nm from the transition of $^8S-^6P$ of Gd^{3+}.

3.5. Energy transfer between Pb^{2+} and Dy^{3+}

The emission spectrum of Pb^{2+} was overlapped with the excitation bands of Dy^{3+} ion, which was a necessity for energy transfer from Pb^{2+} to Dy^{2+} ion. In a doubly doped Dy^{3+} and Pb^{2+} phosphor with a fixed Dy^{3+} concentration, an excitation band in the range of 250–300 nm belonging to the excitation band of Pb^{2+} appeared (shown in Fig. 10). It showed that Pb^{2+} ion could partly transfer its excitation energy to Dy^{3+} ion. The change of Dy^{3+} ion emission intensity with the concentration of Pb^{2+} is shown in Fig. 11. It had its maximum intensity at $X_{Pb}=0.036$. Codoping Gd^{3+} with the above ions could improve the fluorescence intensity of Dy^{3+}. Radiating at 268 nm, the Gd^{3+} and Pb^{2+} excited together. With the increased concentration of Gd^{3+}, the fluorescence intensity of Dy^{3+} increased and that of Pb^{2+} decreased. This phenomena shows that Pb^{2+} transfers its excitation energy to Dy^{3+} through the sublattice of Gd^{3+} ions. With the optimum concentrations of Dy^{3+}, Pb^{2+} and Gd^{3+}, this compound may emit strong white light in a single matrix.

Table 1
Emission wavelength of $Na_{(1-x)}Pb_xRe_9SiO_6O_{26}$

	Y^{3+}	Gd^{3+}	La^{3+}
Wavelength (nm)	384	417	328
Radius at nine coordination (pm)	107.5	110.7	121.6

4. Conclusion

Oxyapatite $NaY_9Si_6O_{26}$ was synthesized by the sol–gel method. By using different silicon source and other reactants, the forming energy of the mixed phases was changed and a pure phase compound could be prepared. The luminescence properties of Eu^{3+}, Tb^{3+}, and Pb^{2+} ion were investigated. Rare earth ions occupy the two sites (6*f* and 4*h*). Dy^{3+} ions could emit white light in this compound, and Pb^{2+} and Gd^{3+} increased its intensity of white light.

Acknowledgements

We acknowledge financial aid from 973 National Key Project for Fundamental Research of Rare Earth Functional Materials; National Noble Youth Sciences Foundation of China (No. 29225102); National Natural Science Foundation of China (No. 29731010, No. 29971030).

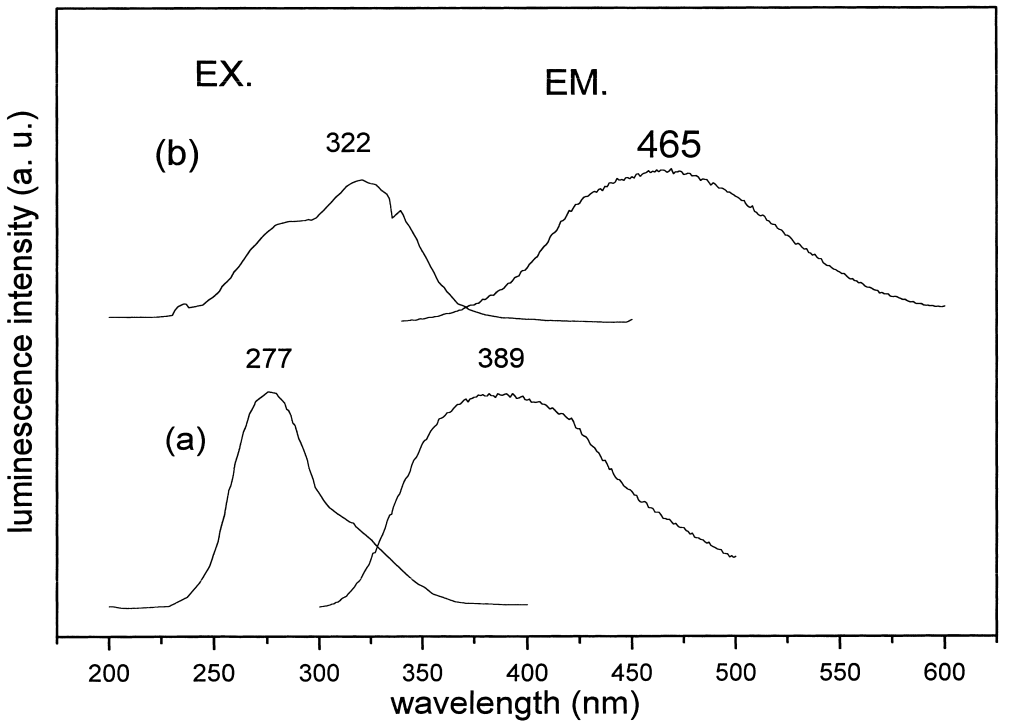

Fig. 8. Luminescence spectra of $NaY_{9(1-x)}Pb_{9x}Si_6O_{26}$ ($x=0.034$) (a) the excitation curve is for emission at 387 nm and the emission curve for excitation at 277 nm. (b) The excitation spectrum is recorded for emission wavelength at 340 nm. The emission spectrum is recorded for excitation wavelength at 322 nm.

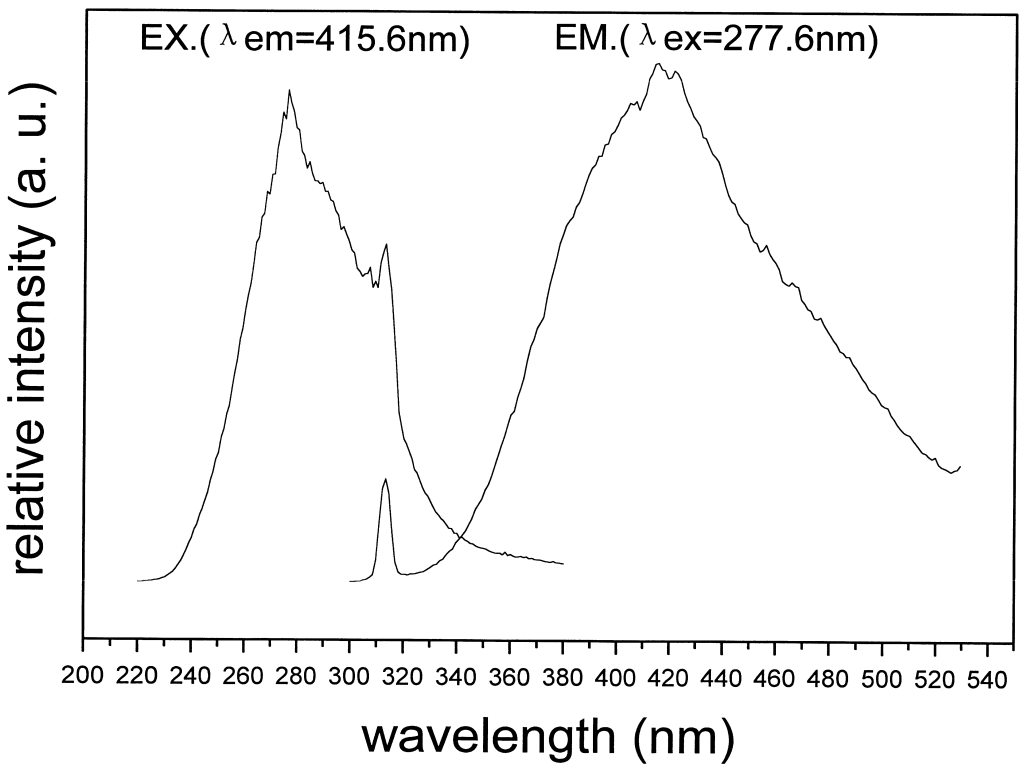

Fig. 9. Excitation and emission spectra of $NaGd_9Si_6O_{26}:Pb^{2+}$ (1at.%).

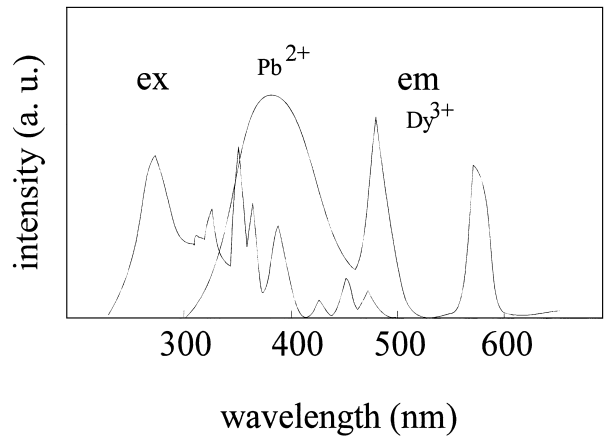

Fig. 10. Fluorescence spectra of doubly doped with Pb^{2+} and Dy^{3+} $NaY_{9(1-x-y)}Pb_{9x}Dy_{9y}Si_6O_{26}$ ($x=0.034$, $y=0.014$).

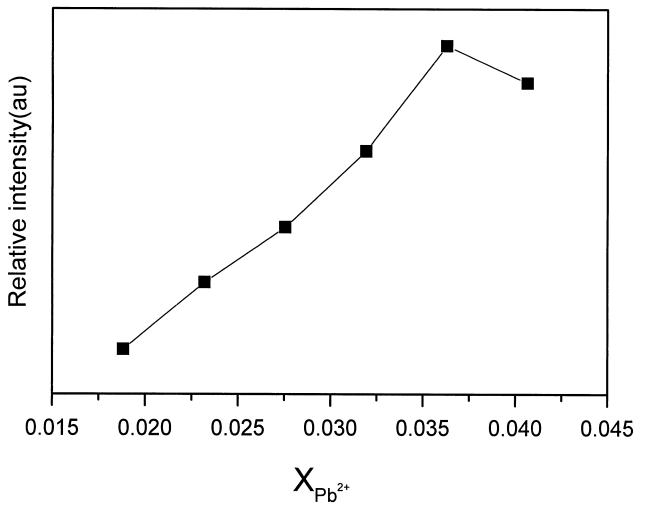

Fig. 11. Change of emission intensity of Dy^{3+} with concentration X of Pb^{2+}.

References

[1] R. Morimo, K. Matae, Mater. Res. Bull. 24 (1989) 175.
[2] E.m. Rabinovich, J. Shmulovich, V.J. Fratello, Am. Ceram. Soc. Bull. 66 (10) (1987) 1505.
[3] R. Morlotti, Mater. Chem. Phys. 31 (1992) 173.
[4] R.G. Pappalardo, J. Walsh, R.B. Hunt, J. Electrochem. Soc. 130 (1983) 2087.
[5] J.P. Budinm, J.C. Michel, F. Auzel, J. Appl. Phys. 50 (1979) 641.
[6] J. Lin, Q. Su, J. Mater. Chem. 5 (4) (1995) 603.
[7] J. Lin, Q. Su, Mater. Res. Bull. 31 (2) (1996) 189.
[8] G. Blass, J. Solid State Chem. 14 (1979) 1821.
[9] S. Asano, N. Yamashita, Phys. Stat. Sol. (b) 108 (1981) 549.